Available online at www.sciencedirect.com
ScienceDirect
Bioorganic & Medicinal Chemistry 16 (2008) 890–901
Bioorganic & Medicinal Chemistry

Design and synthesis of eugenol derivatives, as potent 15-lipoxygenase inhibitors

Hamid Sadeghian,[a] Seyed Mohammad Seyedi,[a,*] Mohammad Reza Saberi,[b,†] Zahra Arghiani[a] and Mehdi Riazi[a]

[a]*Department of Chemistry, Faculty of Sciences, Ferdowsi University of Mashhad, Mashhad 91775-1436, Iran*
[b]*School of Pharmacy, Pharmaceutical Research Center, Mashhad University of Medical Sciences, BuAli Square, Mashhad 9196773117, Iran*

Received 15 August 2007; revised 22 September 2007; accepted 9 October 2007
Available online 12 October 2007

Abstract—A group of 4-allyl-2-methoxyphenol (eugenol) esters were designed, synthesized, and evaluated as potential inhibitors of soybean 15-lipoxygenase (SLO). Compounds **4c**, **4d 4f**, **4p**, and **4q** showed the best IC_{50} in SLO inhibition (IC_{50} = 1.7, 2.3, 2.1, 2.2, and 0.017 μM, respectively). All compounds were docked into SLO active site and showed that allyl group of compounds is oriented toward the iron atom in the active site of SLO. It is assumed that lipophilic interaction of ligand-enzyme would be in charge of inhibiting the enzyme activity. The selectivity of eugenol derivatives in inhibiting 15-HLOb was also compared with 15-HLOa by molecular modeling and multiple alignment techniques.

1. Introduction

Our interest in eugenol derivatives as lipoxygenase inhibitors emerges from the early work by Naidu and co-workers, in which the 5-lipoxygenase inhibition of this natural compound was reported.[1] It is well documented that mammalian lipoxygenases (LOs) are non-heme iron-containing enzymes responsible for the oxidation of polyunsaturated fatty acids and esters to hydroperoxy derivatives.[2] There are heterogeneous family of enzymes distributed widely throughout the plant and animal kingdoms,[3] and named according to the position at which a key substrate, arachidonic acid (AA), is oxidized. Among the mammalian lipoxygenases involved in the etiology of human disease, 5-lipoxygenase (5-LO) is now well established as a target for reducing the production of leukotrienes (important particularly in asthma).[4] More recently, 15-lipoxygenase (15-LO) has emerged as an attractive target for therapeutic intervention.[5] 15-LO has been implicated in the progression of certain cancers[6,7] and chronic obstructive pulmonary disease (COPD).[8] Evidence for the inhibition of 15-LO in the treatment of vascular disease is, however, most compelling.[9] Both transgenic and knockout studies implicate a role for 15-LO in atherogenesis.[10,11] The enzyme is abundantly expressed in macrophages residing within the atherosclerotic lesion.[5] In addition, the immediate products of 15-LO oxidation of AA and linoleic acid (LA) have been shown to be pro-inflammatory[12] and pro-thrombotic.[13]

It is also found that 15-LO is linked to cardiovascular complications due to participation in oxidative modification of low-density lipoproteins (LDL), leading to the development of atherosclerosis.[9]

Conrad and colleagues[15] showed that in vivo 15-LOa has antitumor effects in human airway carcinomas and promotes apoptotic pathway. They showed that neoplastic tissues from human airway carcinomas demonstrated nonspecific staining for human 15-LOa as compared with normal tissues. In contrast, in human prostate tumors 15-LOa was overexpressed as compared with normal adjacent tissue,[7] and 15-LOb was poorly expressed in prostate tumors.[16] In PC3 cells, 13(S)-HODE, one of the 15-LOa metabolites, upregulated MAP kinase, whereas in contrast 15(S)-HETE, the 15-LOb metabolite, downregulated MAP kinase.[17] Taken together, these findings

Keywords: 4-Allyl-2-methoxyphenol; 15-HLOa; 15-HLOb; Protein modeling; Soybean lipoxygenase; Docking.
* Corresponding author. Tel.: +98 05118795162; fax: +98 05118795560; e-mail: smseyedi@yahoo.com
† Tel.: +98 511 7112611; fax: +98 511 7112596.

0968-0896/$ - see front matter © 2007 Elsevier Ltd. All rights reserved.
doi:10.1016/j.bmc.2007.10.016

including the upregulation of 15-LOa within the airway tissue of smoking patients with chronic bronchitis provided new evidence of possible acquired abnormalities linked to airway inflammation. The bronchial epithelium is clearly a key player in inflammation and structural changes in airway diseases. Its rich content in 15-LOa– and 15-LOb–derived products highlights their potential as new target for therapeutic interventions.

Three different strategies have been developed to inhibit the LO's pathway.[18] They involve (i) redox inhibitors or antioxidants, which interfere with the redox cycle of 15-LO, (ii) iron-chelator agents, and (iii) non-redox competitive inhibitors, which compete with AA to bind the enzyme active site.

Eugenol (4-allyl-2-methoxyphenol) is naturally occurring phenolic compound in basil, cinnamon, and nutmeg, and the major component of clove oil. It is widely used as component of zinc oxide eugenol cement in dentistry and is applied to the oral environment.[19] In addition, eugenol is a flavoring agent in cosmetic and food products.[20] Eugenol has been shown to possess many medicinal properties such as antispasmodic,[21] antipyretic,[22] anti-inflammatory,[23] and antibacterial activity.[24] Recently it is reported that eugenol inhibits 5-LO enzyme by non-competitive mechanism.[1]

In this work, seventeen ester derivatives of eugenol **4a**–**q** were designed, synthesized and their activities were identified as the mean of IC_{50} on soybean 15-LO (SLO). There is reasonable homology between the soybean LO and the human one (Fig. 1). This homology becomes more identical (~50%) within 8Å in the active site pocket. Obviously soybean enzyme is much more accessible than the human one. Therefore, one can expect that the results can be extendable to human LO.

In this study, (i) common bonding model of 4-allyl-2-methoxyphenyl carboxylates in SLO active site,

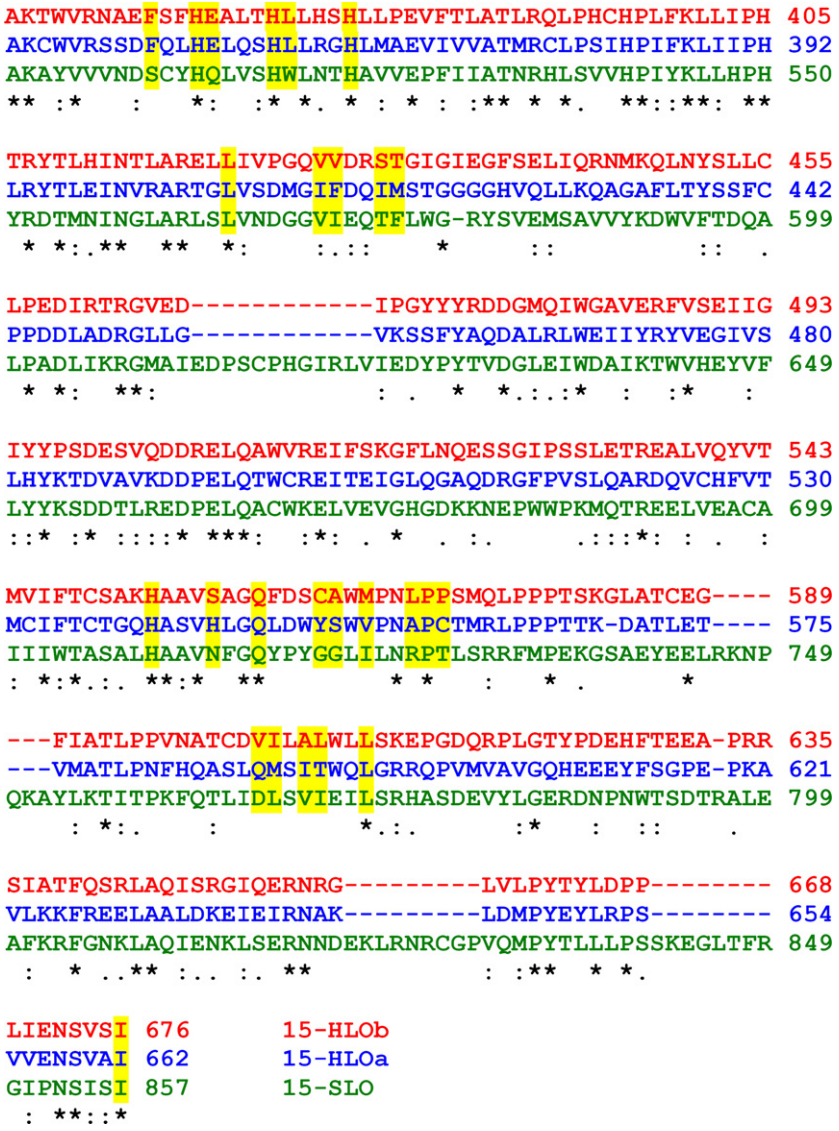

Figure 1. Clustal X (1.81) multiple alignment of SLO (green), 15-HLOa (blue), and 15-HLOb (red). The amino acids in the active site pocket within 8 Å are highlighted by yellow background.

(ii) QSAR study of inhibitors to propose key features of this class of inhibitors, and (iii) theoretical potency of some of these compounds for inhibiting 15-HLOa and 15-HLOb activity are reported.

2. Chemistry

4-Allyl-2-methoxyphenyl esters **4a**–**q** (Scheme 1 and Table 1), according to the literature,[21] started from eugenol **2** and corresponding acid chlorides **3a**–**q** which were either purchased or prepared (**3b**–**d** and **3q**) by reaction of thionyl chloride and corresponding carboxylic acids.[25] All desired esters were synthesized by the action of acid chlorides in either aqueous solution of sodium 4-allyl-2-methoxyphenolate (**4a**, **e**–**q**) or hydrochloride salts of pyridine carboxyl chloride **3b**–**d** (prepared from pyridine carboxylic acids and thionyl chloride) in dry pyridine.

Structural assignments of compounds **4a**–**q** were based upon the spectral and microanalytical data.

3. Molecular modeling, docking, and QSAR study

3.1. Multiple alignment

Highly conserved amino acids were identified through multiple alignment on clustalX 1.81[26] software. Sequences of lipoxygenase (LO) family were selected from blasted sequences via ExPASY proteomics server[27] with *E*-value < 0.02. Multiple alignment process was then carried out on the selected sequences (protein weight matrix: BLOSUM series, gap penalty = 10%).

3.2. Structure optimization

Structures **4a**–**q** were simulated in chem3D professional; Cambridge software; using MM2 method (RMS gradient = 0.05 kcal/mol).[28] Output files were minimized under semi-empirical AM1 method in the second optimization (Convergence limit = 0.01; Iteration limit = 50; RMS gradient = 0.05 kcal/mol; Fletcher-Reeves optimizer algorithm) in HyperChem7.5.[29,30]

Crystal structure of soybean lipoxygenase-3 (arachidonic acid 15-lipoxygenase) complex with 13(S)-hydroperoxy-9(Z)-2,11(E)-octadecadienoic acid was retrieved from RCSB Protein Data Bank (PDB entry: 1IK3).

3.3. Molecular docking

Automated docking simulation was implemented to dock **4a**–**q** into the active site of SLO with AutoDock version 3.03[31] using Lamarckian genetic algorithm.[32] This method has been previously shown to produce bonding modes similar to the experimentally observed modes.[30,32–34] The torsion angles of the ligands were identified, hydrogens were added to the macromolecule, bond distances were edited, and solvent parameters were added to the enzyme 3D structure. Partial atomic charges were then assigned to the macromolecule as well as ligands (Gasteiger for the ligands and Kollman for the protein).

The regions of interest of the enzyme were defined by considering Cartesian chart 18.5, −2.0, and 20.4 as the central of a grid size of 40, 50, and 40 points in X, Y, and Z axises. The docking parameter files were generated using Genetic Algorithm and Local Search Parameters (GALS) while number of generations was set to 50. Compounds **4a**–**q** were each docked into the active site of LO enzyme and the simulations were composed of 50 docking runs, each of 50 cycles containing a maximum of 10,000 accepted and rejected steps. The simulated annealing procedure was started at high temperature (RT = 616 kcal/mol, where R is the gas constant and T is the steady-state temperature) and was decreased by a fraction of 0.95 on each cycle.[33] The 50 docked complexes were clustered with a root-mean-square deviation tolerance of 0.1 Å. The program generated 50 docked conformers of **4a**–**q** corresponding to the lowest-energy structures. After docking procedure

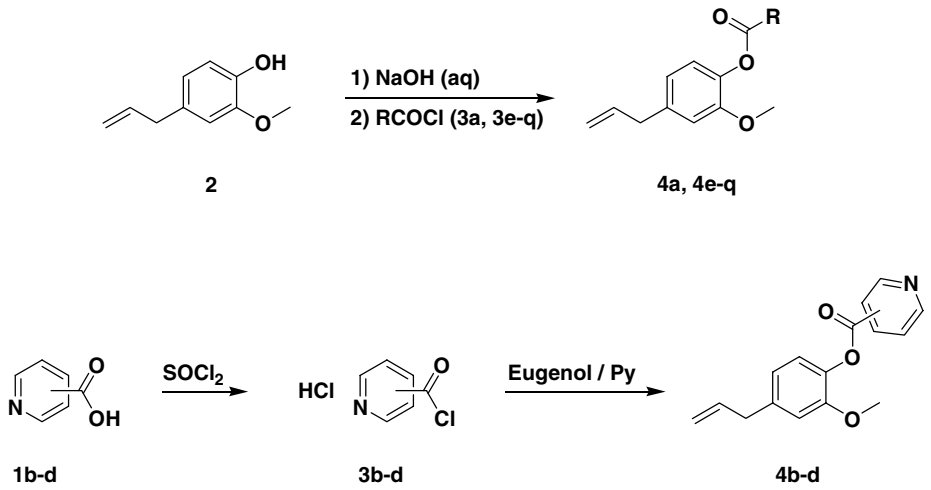

Scheme 1.

Table 1. For **4a**, **4p**, and **4q** the IC_{50} values were calculated from dose–response curves and values are given as means ± SEM of three individual samples

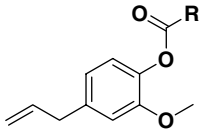

Compound	Structure	IC_{50} (μM)
Eugenol		34.6 ± 1.1
4a		4.4 ± 0.3
4b		33.3 ± 1.5
4c		1.7 ± 0.05
4d		2.3 ± 0.2
4e		6.7 ± 0.8
4f	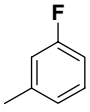	2.1 ± 0.4
4g	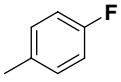	7.2 ± 0.5
4h	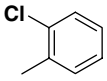	168.0 ± 13.5
4i	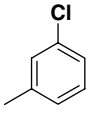	5.2 ± 0.2
4j	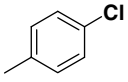	134.3 ± 7.5
4k	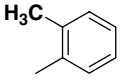	77.2 ± 5.1
4l	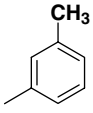	11.4 ± 1.1
4m	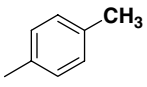	14.6 ± 1.0

Table 1 (*continued*)

Compound	Structure	IC_{50} (μM)
4n	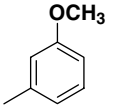	23.0 ± 1.3
4o	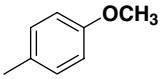	19.0 ± 1.3
4p		2.2 ± 0.3
4q	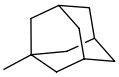	0.017 ± 0.001

in AD3, docking results were submitted to Weblab Viewerlite 4.0[35] and Swiss-PdbViewer 3.7 (spdbv)[36] for further evaluations. The results of docking processing (ΔG_b: estimated free energy of bonding, ΔG_d: final docked energy, and K_i: estimated inhibition constant) are outlined in Table 2.

3.4. QSAR studies

QSAR studies were performed for optimized compounds **4a**–**q** in DRAGON 2.1.[37] In this study van der Waals volume (Sv)[38] and Moriguchi octanol-water partition coefficient ($\log P$)[38] were determined (Table 2).

3.5. Protein modeling

Three-dimensional models of the 15-HLOa and 15-HLOb sequences were constructed by homology modeling. BLAST sequence homology searches were performed in order to identify the template proteins. The soybean lipoxygenase3 complex with linoleic acid (PDB entry: 1IK3) was chosen as the template for modeling the proteins. Model building was performed in the program MODELLER9v1[39] using model-ligand algorithm. Several models at various refinement levels were generated and finally the refined structures involving linoleic acid in the active site pocket were minimized under molecular mechanic AMBER method (RMS gradient = 1) in HyperChem7.5.[29] All models were validated using the program ERRAT at UCLA.[40] The best model had an Errat score of 78–82%.

4. 15-LO inhibitory assessment

Lipoxygenase activity was measured in borate buffer solutions (0.1 M, pH 9) using the method described in the literature,[41,42] by measuring the absorbance at 234 nm for 60 s after addition of the enzyme (soybean 15-lipoxygenase), and linoleic acid (final concentration: 134 μM) as substrate at 20 ± 1 °C. The final enzyme concentration was 167 U/mL. Synthesized substances were added in DMSO solutions (final DMSO concentra-

Table 2. Data obtained from docking and QSAR analyses

Compound	K_i	ΔG_b	ΔG_d	Sv	log *P*
4a	2.09e-6	−7.75	−9.49	7.79	2.255
4b	2.57e-6	−7.63	−8.66	7.19	0.860
4c	3.06e-6	−7.52	−9.34	7.19	0.860
4d	4.70e-6	−7.27	−8.62	7.19	0.860
4e	2.20e-6	−7.72	−9.46	7.90	2.702
4f	1.39e-6	−7.99	−9.78	7.90	2.702
4g	1.68e-6	−7.88	−9.33	7.90	2.702
4h	2.37e-4	−4.94	−3.65	8.53	2.786
4i	7.22e-7	−8.38	−9.17	8.53	2.786
4j	1.58e-6	−7.91	−9.79	8.53	2.786
4k	4.88e-6	−7.25	−9.03	9.39	2.871
4l	6.14e-7	−8.47	−10.29	9.39	2.871
4m	8.61e-7	−8.27	−10.19	9.39	2.871
4n	1.09e-6	−8.13	−10.07	9.90	1.859
4o	8.41e-7	−8.29	−10.25	9.90	1.859
4p	5.78e-7	−8.51	−9.38	9.59	3.516
4q	9.13e-9	−10.97	−12.31	14.78	4.823

ΔG_b, estimated free energy of bonding; ΔG_d, final docking energy, and K_i, estimated inhibition constant; Sv, van der Waals volume of benzene derivatives; log *P*, Moriguchi octanol–water partition coefficient.

tion 1%); whereas DMSO was added in control experiments with no inhibitor. The mixture of each inhibitor and linoleic acid was set as blank sample in testing step. At least six control test tubes and three tubes for each inhibitor solution were measured. To ensure constant enzyme activity throughout the experiment, the enzyme solution was kept in ice, and controls were measured at regular intervals. Calculation of enzyme activity was carried out as previously described[42] and IC_{50} values were determined by linear interpolation between the points around 50% activity (Table 1).

5. Results and discussion

By considering Naidu's work[1] we tested the inhibitory property of eugenol on the SLO (substrate: linoleic acid). The results showed IC_{50} = 34.6 μM for the mentioned enzyme. Since a non-competitive mechanism has been proved for inhibitory activity of eugenol in inhibition of 5-LO,[1] we thought the mechanism might go through oxidation of hydroxyl group which mimics the fact of non-competitive theory reported by Naidu.[1] To prove this idea the hydroxyl group was protected by benzoate (a bulky and moderately lipophilic group). Unexpectedly the benzoate analog **4a** showed a better activity (IC_{50} = 4.4 μM) which means that the activity still exists and no other products such as hydroperoxy are isolated from action of the LO enzyme on **4a** as substrate (assuming that hydroperoxy is supposed to be obtained if the redox pathway is blocked and the inhibitor acts through its allylic group in reaction with the enzyme active site similar to the oxidation of natural unsaturated fatty acids).[‡]

[‡] Twenty milligrams of substrate was reacted with soybean LO enzyme (1000 U/mL) in 30 mL borate buffer solution (0.1 M, pH 9) at 20 °C for 1 h. The mixture was then extracted with dichloromethane (2 × 15 mL) and analyzed by TLC.

Regarding the site-directed mutagenesis reported by Klinman, Minor, and Holman[43,44] and docking procedure in this study, one might conclude that eugenol is able to inhibit LO through allyl interaction with amino acids close to iron atom of the enzyme, mimicking enzymic natural substrate (i.e., unsaturated fatty acid).

Benzoate and cycloalkylate analogs **4b–q** were designed, synthesized, and docked into the active site to support this mechanism. The esters of 4-allyl-2-methoxyphenol **4a–q** showed a broad range of inhibition activity on the enzyme (IC_{50} = 0.017–168.0 μM; Table 1). Compound **4q** having an adamantanecarboxylate substituent was the most potent inhibitor at 17 nM, while the nicotinate, 3-fluorobenzoate, cyclohexanecarboxylate, and isonicotinate analogs (**4c**, **4f**, **4p**, and **4d**, respectively) presented less activity (IC_{50} = 1.7, 2.1, 2.2, and 2.3 μM, respectively). It was interesting to view 2- and 4-chlorobenzoate analogs (**4h** and **4j**) as weak inhibitors of SLO (IC_{50} > 100 μM).

The experimental results matched with theoretical K_i of docking study for those models (Table 2) in which allylic double bond oriented toward iron atom similar to orientation of linoleic acid (LA) in the active site (Figs. 2 and 3).[43] We generated 50 docked conformers of **4a–q** corresponding to the lowest energy structures in ADT software. A detailed inspection of each independent inhibitor conformer revealed that more than 40% of docking results had nearly identical orientations in which allyl group of each inhibitor oriented toward Fe core (except compounds **4h**, **4i**, **4k**, and **4j**: <20%). One conformer from each ester cluster which had more similarity with optimum conformer (lowest *K*i) of benzoate analog (**4a**) was adopted as the 'consensus' structure and used for further analysis.

It seems that the allyl group and phenyl core have hydrophobic interaction with Ile^{557}, Leu^{565}, Leu^{773},

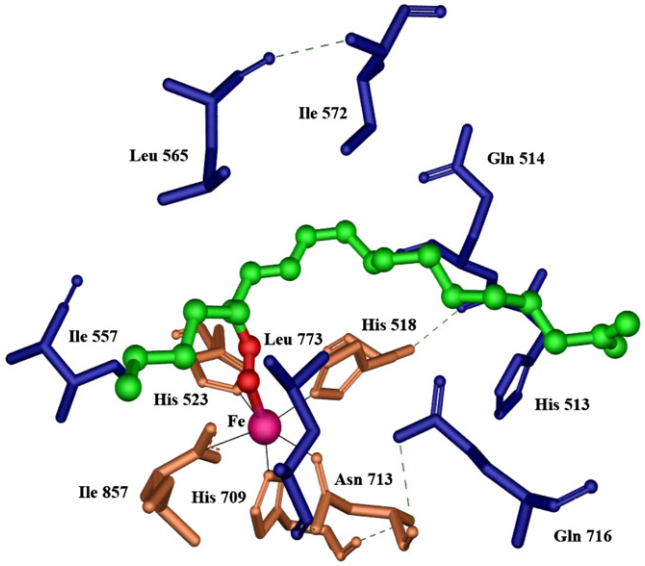

Figure 2. X-ray presentation of SLO active site pocket complex with 13(S)-hydroperoxy-9(Z)-2,11(E)-octadecadienoic acid (green ball and stick) (PDB entry: 1IK3). The conserved amino acids are presented in blue and light brown color. Hydrogen bonds are shown by dashed black lines.

and Ile^{572}, respectively, in such an orientation. The most critical residues, that is, Ile^{557}, Leu^{565}, Leu^{773}, and Ile^{572}, surprisingly appeared close to the active site (Fig. 2). X-ray presentation of LA into SLO[43] indicates that Ile^{557}, Leu^{565}, and Leu^{773} lay within 4–6 Å of Fe^{3+}-OH and both Leus are near the reactive C-11–C-13 of LA (C-11: hydrogen abstraction site, C-13: oxygenation site). Although Ile^{572} is far from Fe^{3+}-OH (at 9 Å), still forms part of the substrate-bonding cavity. Each of these residues provides a large surface to interact with natural substrate, particularly Leu^{565} and Leu^{773}. Mutating large residues such as Ile or Leu to an Ala opens up space within the bonding pocket of SLO, leading to altered $H^{\cdot}$ transfer kinetics. The $Ile^{557} \rightarrow Ala$ and $Ile^{572} \rightarrow Phe$ mutants decreased k_{cat} by twofold from WT (wild type), While $Leu^{565} \rightarrow Ala$ and $Leu^{773} \rightarrow Ala$ decreased k_{cat} by 60- and 1000-fold, respectively, indicating that these hydrophobic residues (specially Leu^{565}, and Leu^{773}) contribute significantly to catalysis.[44] According to the result of multiple alignment, three amino acids Ile^{557}, Leu^{565}, and Leu^{773} are found to be conserved over all species.

We can also view in Figures. 3 and 4 that the proposed orientation of docked molecules has hydrophilic and hydrophobic interaction with conserved His^{513}, Gln^{514}, and Gln^{716}. The amino acids Gln^{514} and Gln^{716} play a key role in oxidation potential of Fe^{3+} via hydrogen bonding with Asn^{713} and His^{518}.[45] This hydrogen bond network is present in both SLO and 15-RLO (rabbit 15-LO) structures and also plays a steric role in orienting the substrate and inhibitor bound to LO.[45] The C-3–C-8 hydrocarbon tail of LA is flanked by the hydrophobic portion of the Gln^{514} and Gln^{716} (Figs. 2 and 4). Disrupting this bonding pocket by changing the position of Gln^{514} and Glu^{716} may affect the proper positioning of the substrate for C-H bond cleavage so that abstraction becomes more rate-limiting (as was observed in the $Gln^{514} \rightarrow Ala$, $Gln^{716} \rightarrow Asn$ and $Gln^{716} \rightarrow Glu$ mutants by 4-, 3-, and 6-fold decrease in k_{cat} from WT SLO, respectively,[45]). Proposed inhibitory model of docked molecules has hydrogen bond with Gln^{716} via carbonyl group (Fig. 3). This can change the oxidation potential of ferric ion by disrupting the hydrogen bond of Gln^{716} and Asn^{713}. The aromatic and aliphatic part of carboxylate moiety in eugenol derivatives is flanked by the hydrophobic portion of the Gln^{716} side chain like LA (Fig. 4).

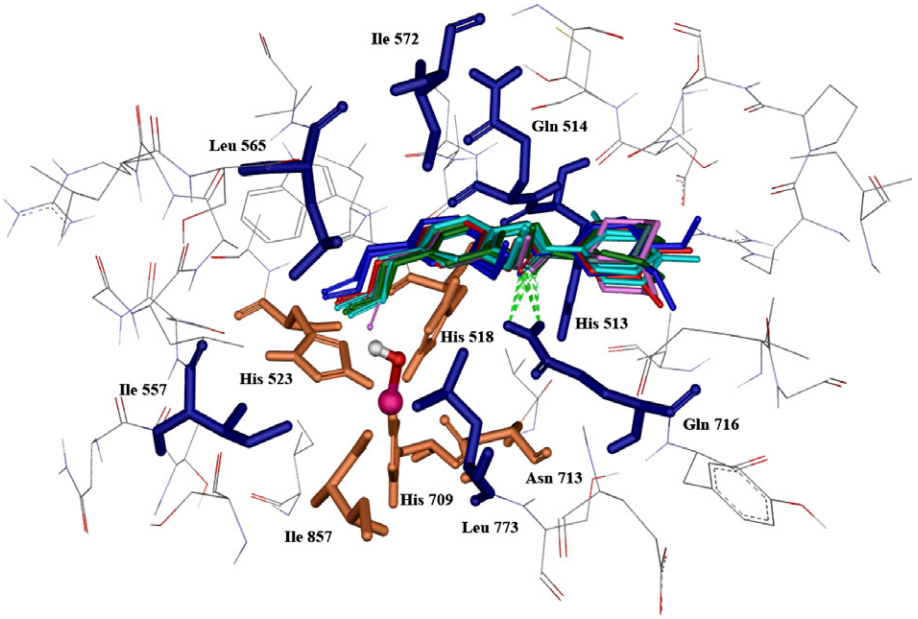

Figure 3. Superimposition of the bonding conformations of **4a**–**q** in colored stick in the active site of SLO within 8 Å. The hydrogen bonds between Gln^{716} and inhibitors are shown by dashed green lines.

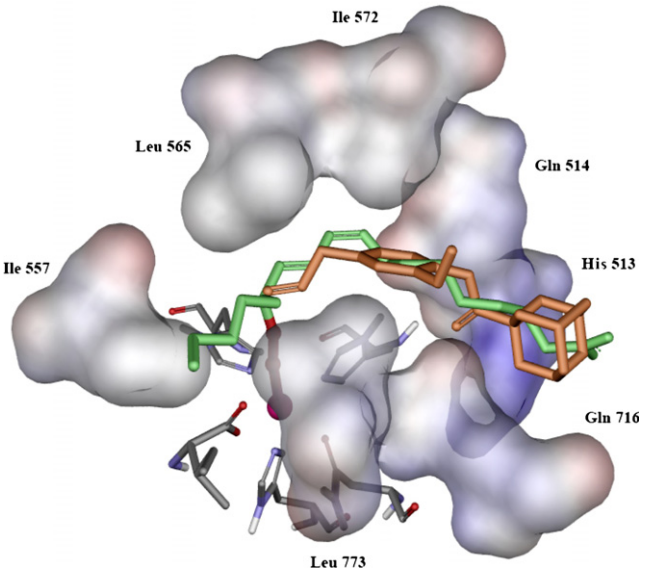

Figure 4. Solvent surface view of conserved amino acids which have interaction with 13(S)-hydroperoxy-9(Z)-2,11(E)-octadecadienoic acid (green stick) and **4q** (light brown stick).

The K_i of proposed model of compounds, **4a**, **4p**, and **4q**, have good relation with IC_{50} results (Fig. 5). This comes from tendency of the carboxylate moiety for filling all of the empty lipophilic space of Val^{372}, Phe^{576}, Ile^{770}, and Gln^{716} side chains (Fig. 6). This result can be clarified by considering lipophilic factor ($\log P$) and van der Waals volume (Sv) of cyclohexyl, phenyl, and adamantyl groups (Table 2).

It is notable that in each group of isomeric inhibitors, the compounds with substituent or heteroatom in position 2 have lower activity in comparison with other isomers (**4h**, **4k**, and **4b**: IC_{50} = 168.0, 77.2, and 33.3 μM, respectively). Compound **4e** (IC_{50} = 6.7 μM) does not follow the above road map probably because of the hydrogen bonding of fluorine with conserved His^{513} (Fig. 7). Comparison of the calculated 1D-QSAR data with IC_{50} values, showed linear and non-linear relation between Sv and IC_{50} values of inhibitors with substituent or heteroatom at *para* and *meta* position, respectively (Fig. 8a and b—compound **4j** was excluded because of high deviation). Decreasing of Sv increases tendency of these compounds in SLO inhibition.

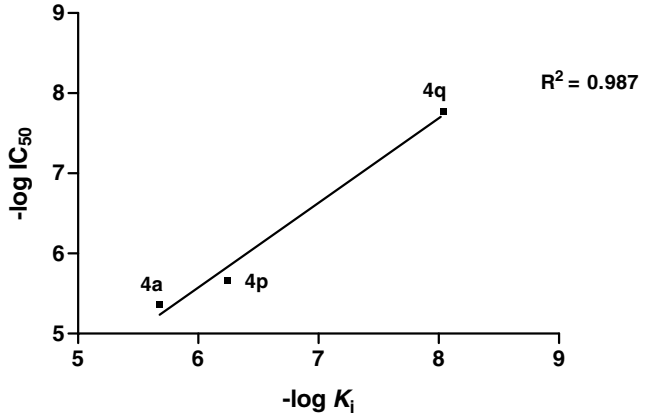

Figure 5. Diagram of $-\log IC_{50}$ versus $-\log K_i$ for compounds **4a**, **4p**, and **4q**.

Due to lipophilic interaction area of carboxylate moiety (Sv and $\log P$) in inhibition of SLO activity, we studied the tendency of compounds **4a**, **4p**, and **4q** for inhibiting modeled 15-HLOa and 15-HLOb (these compounds showed good relation between K_i and IC_{50} variations for SLO). The structures of modeled 15-HLOa and 15-HLOb demonstrate a high level of conservation of the overall topology. Thus the structures of 15-HLOa could be superimposed on the 15-HLOb with RMS for the C-α atoms of around 0.95Å. The largest differences between the 15-HLOa and 15-HLOb were found in the regions of helix α2, α4-α5, α6-α7, and α15-α16 (residues 141–152, 190–197, 233–246, 257–259, 321–327, and 565–571 for 15-HLOa in contrast with 155–165, 204–207, 243–247, 258–273, 336–339, and 578–588 for 15-HLOb, respectively). These residues do not build up any part of the substrate binding cleft. In the active site pocket of the two modeled proteins, the backbone of conserved amino acids laying within 8 Å of the Fe atom is well fitted but this is not observed for other conserved amino acids in this region. Free space of catalytic pocket seems to be smaller for 15-HLOa in comparison with 15-HLOb. This lacking comes from steric occupation of aromatic side chains of Phe^{352}, Phe^{414}, and Tyr^{551} in the cavity (Fig. 9b). After docking process on the modeled enzymes, **4q** showed better K_i for 15-HLOb than 15-HLOa by 100-fold in the same orientation which had been proved for SLO (Table 3 and Fig. 9). It may have something to do with the smaller space of active site pocket of 15-HLOa in comparison with 15-HLOb. Considering the lipophilicity of amino acids which surrounded the carboxylate moiety of inhibitors, these amino acids are more lipophilic in 15-HLOb in comparison with 15-HLOa (Table 4). The lipophilicity was taken from ExPASy[27] (ProtScale) by applying Hphob (Kyte and Doolittle hydropathicity).[46] Therefore, we assume **4q** a selective inhibitor for 15-HLOb in comparison with 15-HLOa.

In summary, the present study introduces that large and lipophilic eugenol esters such as **4q** can behave as SLO inhibitors (IC_{50} = 17 nM) and also as a selective inhibitor of 15-HLOb when compared with 15-HLOa. The importance of these compounds could be more highlighted when we rank their easy synthesis pathway and their high yield.

6. Experimental

6.1. General procedures

Melting points were recorded on an Electrothermal type 9100 melting point apparatus. The ^1H NMR (100 MHz) spectra were recorded on a Bruker AC 100 spectrometer. Elemental analysis was obtained on a Thermo Finnigan Flash EA microanalyzer. All measurements of lipoxygenase activities were carried out using an Agilent 8453 spectrophotometer. The soybean 15-lipoxygenase

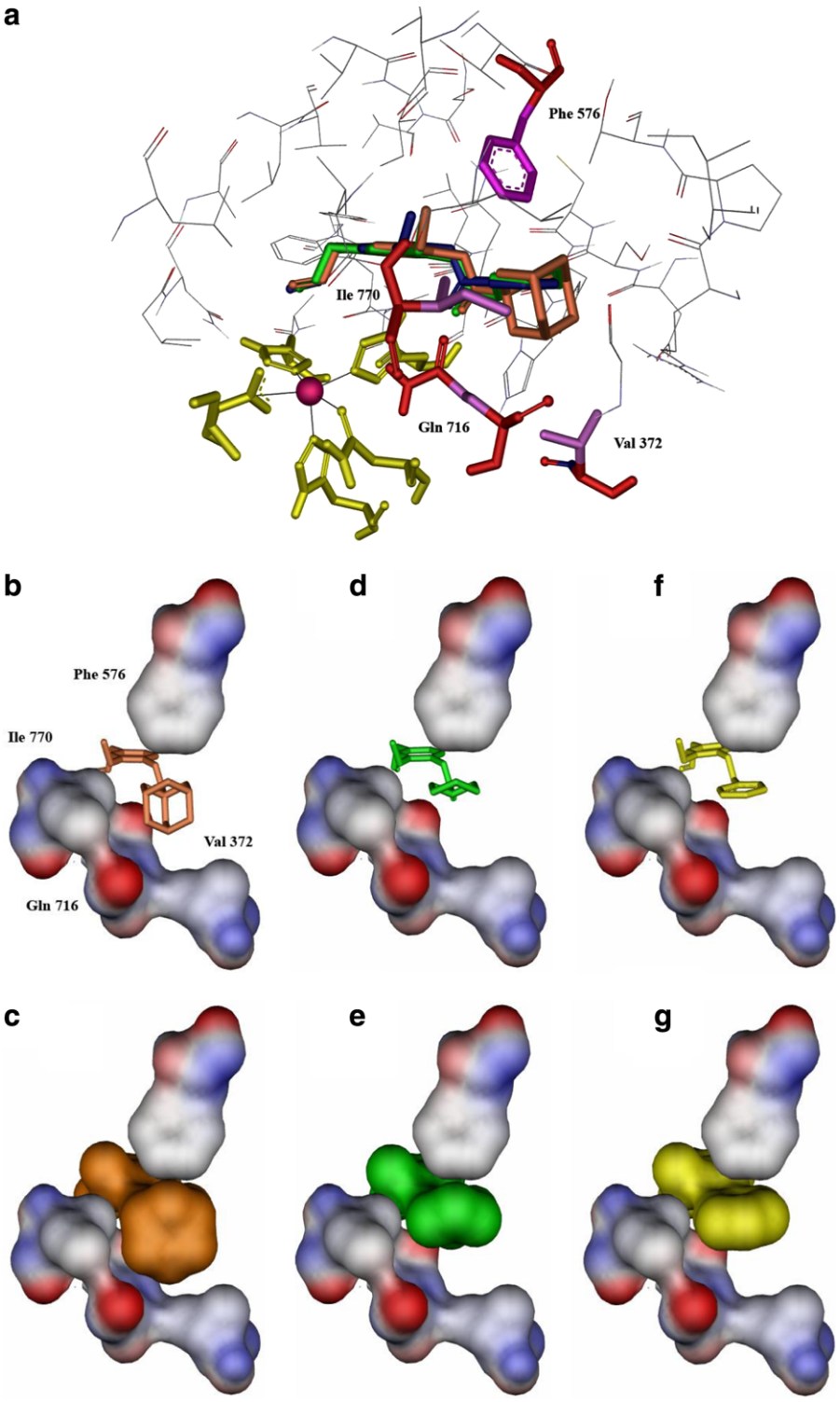

Figure 6. (a) Amino acids having lipophilic interaction with **4a**, **4p**, and **4q** (The lipophilic parts of the side chains are distinguished by purple color). Solvent surface of lipophilic amino acids interacting with carboxylate moiety of **4q**, **4p**, and **4a** is shown in b, c, d, e, f, and g, respectively.

and other chemicals were purchased from Sigma, Fluka, and Merck Co., respectively.

6.2. General procedure for preparation of 4-allyl-2-methoxyphenyl carboxylate 4b-d

Thionyl chloride (10 mL) was added to pyridine carboxylic acids **1b–d** (20 mmol, 2.46 g). The mixture was stirred and refluxed for 1 h. The thionyl chloride was then evaporated under reduced pressure giving a white crystalline residue of hydrochloride of **3b–d**. The purity of **3b–d** was quite sufficient to use the product directly for the following synthesis.

To a stirred solution of **3b–d** (1.78 g, 10 mmol) in dry pyridine (10 mL) was added eugenol (1.64 g,

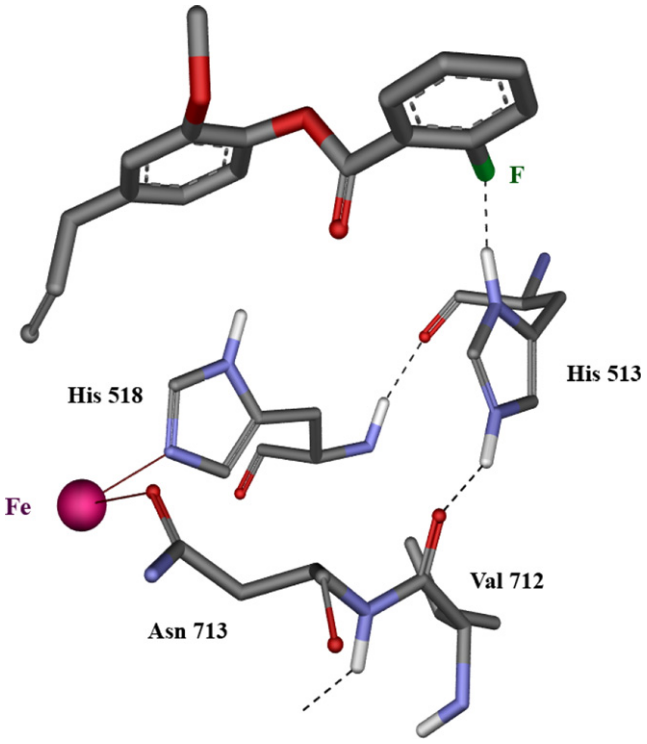

Figure 7. Stick view of compound **4e** interacting with His[513] via hydrogen bonding of fluorine atom (green color). Hydrogen bonds are revealed by dashed black lines.

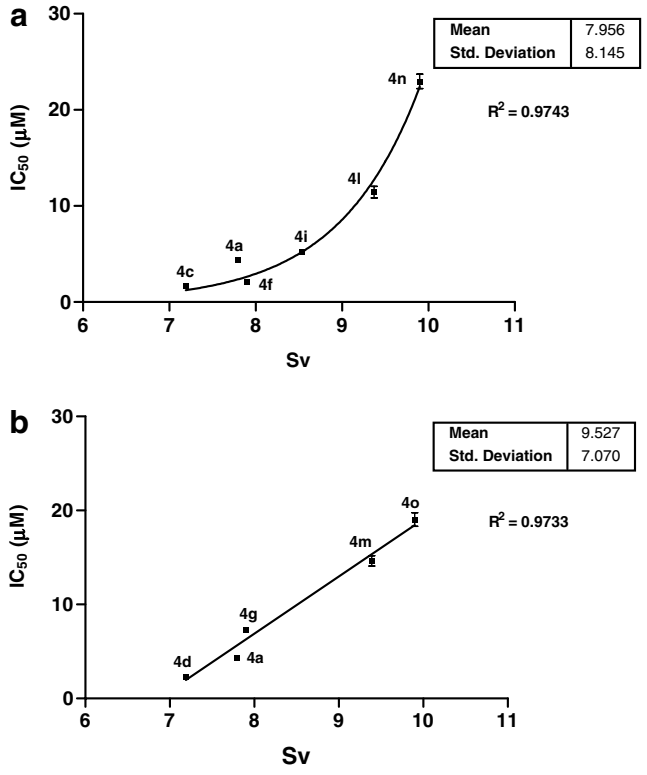

Figure 8. Diagrams of measured IC_{50} versus van der Waals volume (Sv) of benzoate moiety of eugenol esters with *meta* (a) and *para* (b) substituent.

10 mmol) dropwise at room temperature. The mixture was refluxed in oil bath while stirring for 4 h. After reaction completion, the pyridine was evaporated under reduced pressure. The residue was treated with 5% sodium carbonate (15 mL) and extracted with dichloromethane (2 × 15 mL). The organic extract was dried with anhydrous sodium sulfate, concentrated under reduced pressure, and crystallized from ethanol to provide the pure desired compounds **4b–d**.

6.3. General procedure for preparation of 4-allyl-2-methoxyphenyl carboxylate 4a and 4e-q

The acid chlorides **1a**, **e–q** were synthesized via the method described for compounds **2b–d**.

To a stirred solution of sodium hydroxide (0.48 g, 12 mmol) and eugenol (1.64 g, 10 mmol) in water (10 mL) were added acid chlorides **3a** and **3e–q** (10 mmol) dropwise at room temperature. After 30-min stirring at room temperature the mixture was extracted with dichloromethane (2 × 15 mL), washed with 5% sodium carbonate (2 × 15 mL), dried with anhydrous sodium sulfate, and concentrated under reduced pressure to provide the desired compounds. All products were crystallized from ethanol except **4h** and **4k** which were purified by column chromatography (silica gel 60; 230–400, eluent: chloroform).

6.3.1. 4-Allyl-2-methoxyphenyl benzoate (4a). White crystal. Yield: 87%; mp 55–56 °C. IR: 1727 cm^{-1} (C=O). ^1H NMR ($CDCl_3$): δ 3.45 (d, 2, J = 6.6 Hz, $-CH_2-$), 3.80 (s, 3, $-OCH_3$), 5.01–5.25 (m, 2, $H_2C=$), 5.80–6.25 (m, 1, =CH), 6.82 (d, 1, J = 8.4, H-5), 6.85 (s, 1, H-3), 7.10 (d, J = 8.4, H-6), 7.40–7.72 (m, 3, H-3′, H-4′, H-5′), 8.22 (d, 2, J = 7.9, H-2′, H-6′). Found C, 76.21; H, 6.03. $C_{17}H_{16}O_3$ requires: C, 76.10; H, 6.01%.

6.3.2. 4-Allyl-2-methoxyphenyl 2-pyridinecarboxylate (4b). Light brown crystal. Yield: 43%; mp 90–91 °C. IR: 1754 cm^{-1} (C=O). ^1H NMR ($CDCl_3$): δ 3.42 (d, 2, J = 6.6 Hz, $-CH_2-$), 3.80 (s, 3, $-OCH_3$), 5.02–5.25 (m, 2, $H_2C=$), 5.72–6.22 (m, 1, =CH), 6.81 (d, 1, J = 8.4, H-5), 6.84 (s, 1, H-3), 7.12 (d, 1, J = 8.4, H-6), 7.54 (m, 1, H-5′), 7.89 (m, 1, H-4′), 8.27 (d, 1, J = 7, H-3′), 8.84 (d, J = 4, H-6′). Found C, 71.04; H, 5.65; N, 5.25. $C_{16}H_{15}NO_3$ requires: C, 71.36; H, 5.61; N, 5.20%.

6.3.3. 4-Allyl-2-methoxyphenyl nicotinate (4c). White crystal. Yield: 71%; mp 70–71 °C. IR: 1745 cm^{-1} (C=O). ^1H NMR ($CDCl_3$): δ 3.42 (d, 2, J = 6.6 Hz, $-CH_2-$), 3.81 (s, 3, $-OCH_3$), 5.02–5.25 (m, 2, $H_2C=$), 5.72–6.22 (m, 1, =CH), 6.81 (d, 1, J = 8.4, H-5), 6.85 (s, 1, H-3), 7.06 (d, J = 8.4, H-6), 7.45 (dd, 1, J = 7.8, 4.9, H-5′), 8.45 (d, 1, J = 7.8, H-4′), 8.82 (d, J = 4.9, H-6′), 9.40 (s, 1, H-2′). Found C, 71.08; H, 5.58; N, 5.19. $C_{16}H_{15}NO_3$ requires: C, 71.36; H, 5.61; N, 5.20%.

6.3.4. 4-Allyl-2-methoxyphenyl isonicotinate (4d). White crystal. Yield: 73%; mp 56–57 °C. IR: 1762 cm^{-1} (C=O). ^1H NMR ($CDCl_3$): δ 3.41 (d, 2, J = 6.5 Hz,

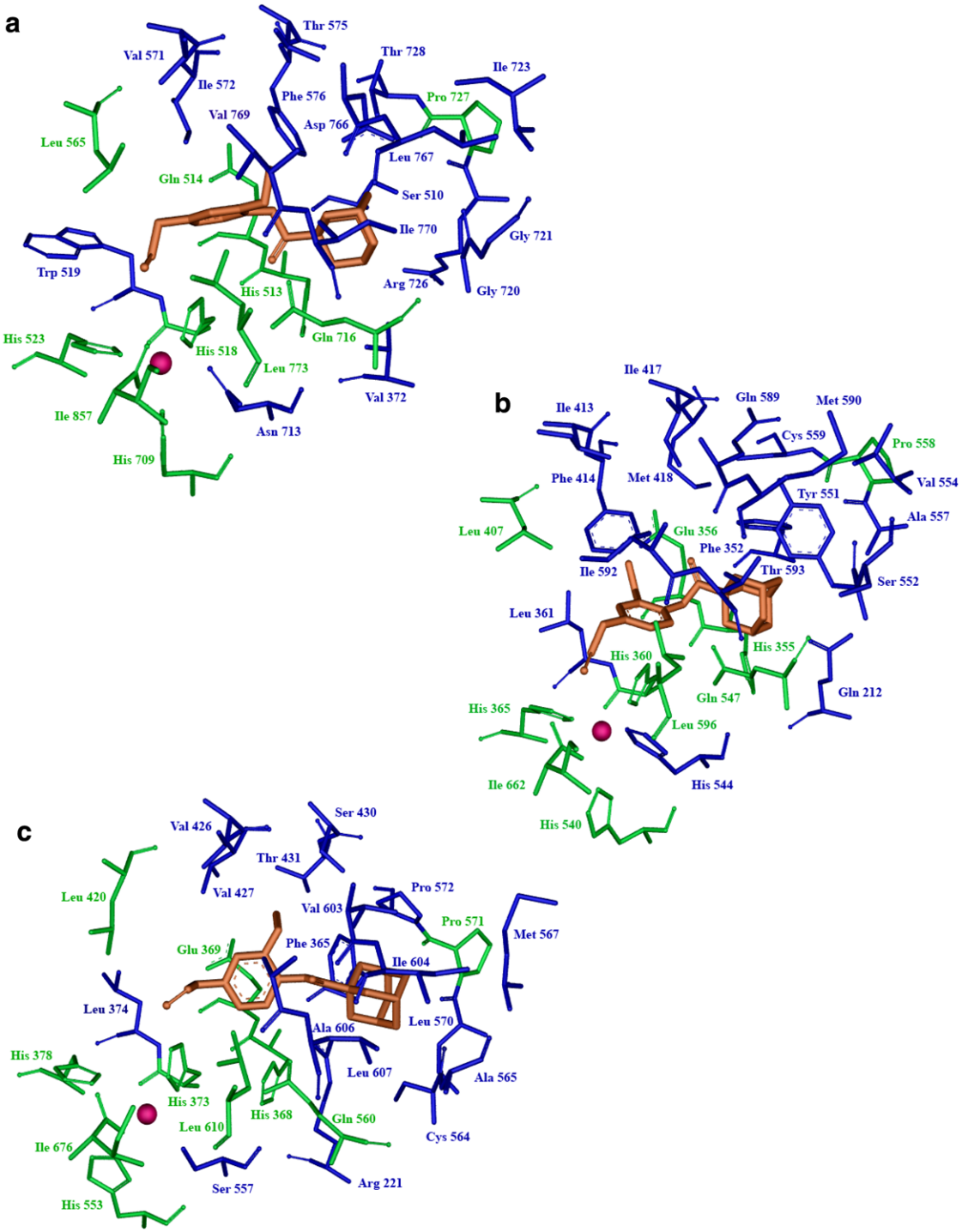

Figure 9. Docking results of **4q** in the active site of SLO (a), 15-HLOa (b), and 15-HLOb (c). The conserved and mutated amino acids are presented by green and blue color, respectively.

Table 3. The estimated inhibition constant (K_i) of **4a**, **4p**, and **4q** from docking study on 15-HLOa and 15-HLOb

Compound	K_i (15-HLOa)	K_i (15-HLOb)
4a	1.90e-6	5.48e-6
4p	6.05e-7	1.86e-6
4q	1.96e-6	3.58e-8

–CH_2–), 3.81 (s, 3, –OCH_3), 5.00–5.27 (m, 2, H_2C=), 5.80–6.20 (m, 1, =CH), 6.85 (d, 1, J = 8.4, H-5), 6.86 (s, 1, H-3), 7.09 (d, J = 8.4, H-6), 8.00 (d, 2, J = 5, H-3′, H-5′), 8.86 (d, 2, J = 5, H-2′, H-6′). Found C, 71.19; H, 5.63; N, 5.22. $C_{16}H_{15}NO_3$ requires: C, 71.36; H, 5.61; N, 5.20%.

6.3.5. 4-Allyl-2-methoxyphenyl 2-fluorobenzoate (4e). Light brown crystal. Yield: 63%; mp 55–56 °C. IR: 1729 cm^{-1} (C=O). ^1H NMR ($CDCl_3$): δ 3.40 (d, 2, J = 6.6 Hz, –CH_2–), 3.81 (s, 3, –OCH_3), 5.01–5.23 (m, 2, H_2C=), 5.77–6.26 (m, 1, =CH), 6.60 (m, 2, H-3′, H-5′), 6.81 (d, 1, J = 8.5, H-5), 6.84 (s, 1, H-3), 7.06

Table 4. The Kyte & Doolittle hydropathicity (Hphob) of amino acids which have direct interaction with carboxylate moiety of inhibitors

15-HLOa	Hphob	15-HLOb	Hphob
Gln^{211}	−3.50	Arg^{221}	−4.50
Phe^{352}	2.80	Phe^{365}	2.80
Gln^{547}	−3.50	Gln^{560}	−3.50
Tyr^{551}	−1.30	Cys^{564}	2.50
Ser^{552}	−0.80	Ala^{565}	1.80
Val^{554}	4.20	Met^{567}	1.90
Ala^{557}	1.80	Leu^{570}	3.80
Pro^{558}	−1.60	Pro^{571}	−1.60
Cys^{559}	2.50	Pro^{572}	−1.60
Gln^{589}	−3.50	Val^{603}	4.20
Met^{590}	1.90	Ile^{604}	4.50
Thr^{593}	−0.70	Leu^{607}	3.80

(d, J = 8.5, H-6), 7.39 (m, 1, H-4′), 7.67 (m, 1, H-6′). Found C, 71.07; H, 5.33. $C_{17}H_{15}FO_3$ requires: C, 71.32; H, 5.28%.

6.3.6. 4-Allyl-2-methoxyphenyl 3-fluorobenzoate (4f). White crystal. Yield: 75%; mp 61–62 °C. IR: 1744 cm^{-1} (C═O). ^1H NMR ($CDCl_3$): δ 3.41 (d, 2, J = 6.5 Hz, –CH_2–), 3.80 (s, 3, –OCH_3), 5.00–5.28 (m, 2, H_2C═), 5.78–6.26 (m, 1, ═CH), 6.81 (d, 1, J = 8.4, H-5), 6.85 (s, 1, H-3), 7.06 (d, J = 8.4, H-6), 7.25–7.52 (m, 2, H-4′, H-5′), 7.96 (m, 2, H-2′, H-6′). Found C, 71.15; H, 5.33. $C_{17}H_{15}FO_3$ requires: C, 71.32; H, 5.28%.

6.3.7. 4-Allyl-2-methoxyphenyl 4-fluorobenzoate (4g). White crystal. Yield: 79%; mp 56–57 °C. IR: 1732 cm^{-1} (C═O). ^1H NMR ($CDCl_3$): δ 3.41 (d, 2, J = 6.5 Hz, –CH_2–), 3.80 (s, 3, –OCH_3), 5.02–5.24 (m, 2, H_2C═), 5.78–6.23 (m, 1, ═CH), 6.81 (d, 1, J = 8.4, H-5), 6.84 (s, 1, H-3), 7.06 (d, J = 8.4, H-6), 7.18 (m, 2, H-3′, H-5′), 8.23 (m, 2, H-2′, H-6′). Found C, 71.17; H, 5.29. $C_{17}H_{15}FO_3$ requires: C, 71.32; H, 5.28%.

6.3.8. 4-Allyl-2-methoxyphenyl 2-chlorobenzoate (4h). Light yellow oil. Yield: 39%. IR: 1741 cm^{-1} (C═O). ^1H NMR ($CDCl_3$): δ 3.41 (d, 2, J = 6.5 Hz, –CH_2–), 3.84 (s, 3, –OCH_3), 5.00–5.26 (m, 2, H_2C═), 5.80–6.25 (m, 1, ═CH), 6.82 (d, 1, J = 8.4, H-5), 6.85 (s, 1, H-3), 7.10 (d, J = 8.4, H-6), 7.20–7.60 (m, 3, H-3′, H-4′, H-5′), 8.11 (d, 1, J = 5.9, H-6′). Found C, 67.73; H, 5.04. $C_{17}H_{15}ClO_3$ requires: C, 67.44; H, 4.99%.

6.3.9. 4-Allyl-2-methoxyphenyl 3-chlorobenzoate (4i). White crystal. Yield: 81%; mp 48–49 °C. IR: 1745 cm^{-1} (C═O). ^1H NMR ($CDCl_3$): δ 3.40 (d, 2, J = 6.5 Hz, –CH_2–), 3.80 (s, 3, –OCH_3), 5.00–5.25 (m, 2, H_2C═), 5.80–6.20 (m, 1, ═CH), 6.80 (d, 1, J = 8.4, H-5), 6.84 (s, 1, H-3), 7.08 (d, J = 8.4, H-6), 7.44 (t, 1, J = 7.6, H-5′), 7.60 (d, 1, J = 7.6, H-4′), 8.09 (d, J = 7.6, H-6′), 8.19 (s, 1, H-2′). Found C, 67.56; H, 4.97. $C_{17}H_{15}ClO_3$ requires: C, 67.44; H, 4.99%.

6.3.10. 4-Allyl-2-methoxyphenyl 4-chlorobenzoate (4j). White crystal. Yield: 88%; mp 82–83 °C. IR: 1743 cm^{-1} (C═O). ^1H NMR ($CDCl_3$): δ 3.40 (d, 2, J = 6.6 Hz, –CH_2–), 3.80 (s, 3, –OCH_3), 5.00–5.26 (m, 2, H_2C═), 5.80–6.20 (m, 1, ═CH), 6.80 (d, 1, J = 8.4, H-5), 6.84 (s, 1, H-3), 7.10 (d, J = 8.4, H-6), 7.50 (d, 2, J = 8.7, H-3′, H-5′), 8.15 (d, 2, J = 8.7, H-2′, H-6′). Found C, 67.49; H, 5.02. $C_{17}H_{15}ClO_3$ requires: C, 67.44; H, 4.99%.

6.3.11. 4-Allyl-2-methoxyphenyl 2-methylbenzoate (4k). Light yellow oil. Yield: 18%. IR: 1727 cm^{-1} (C═O). ^1H NMR ($CDCl_3$): δ 2.45 (s, 3H, –CH_3), 3.39 (d, 2, J = 6.5 Hz, –CH_2–), 3.85 (s, 3, –OCH_3), 5.00–5.20 (m, 2, H_2C═), 5.79–6.23 (m, 1, ═CH), 6.79 (d, 1, J = 8.5, H-5), 6.83 (s, 1, H-3), 7.04 (d, J = 8.5, H-6), 7.22–7.45 (m, 3, H-3′, H-4′, H-5′), 8.08 (d, 1, J = 7.6, H-6′). Found C, 76.83; H, 6.50. $C_{18}H_{18}O_3$ requires: C, 76.57; H, 6.43%.

6.3.12. 4-Allyl-2-methoxyphenyl 3-methylbenzoate (4l). White crystal. Yield: 85%; mp 51–52 °C. IR: 1723 cm^{-1} (C═O). ^1H NMR ($CDCl_3$): δ 2.43 (s, 3H, –CH_3), 3.41 (d, 2, J = 6.5 Hz, –CH_2–), 3.80 (s, 3, –OCH_3), 5.02–5.24 (m, 2, H_2C═), 5.81-6.25 (m, 1, ═CH), 6.81 (d, 1, J = 8.6, H-5), 6.84 (s, 1, H-3), 7.06 (d, J = 8.6, H-6), 7.38 (m, 2, H-4′, H-5′), 8.03 (m, 2, H-2′, H-6′). Found C, 76.70; H, 6.46. $C_{18}H_{18}O_3$ requires: C, 76.57; H, 6.43%.

6.3.13. 4-Allyl-2-methoxyphenyl 4-methylbenzoate (4m). White crystal. Yield: 87%; mp 92–93 °C. IR: 1730 cm^{-1} (C═O). ^1H NMR ($CDCl_3$): δ 2.45 (s, 3, –CH_3), 3.41 (d, 2, J = 6.5 Hz, –CH_2–), 3.81 (s, 3, –OCH_3), 5.00–5.25 (m, 2, H_2C═), 5.80–6.20 (m, 1, ═CH), 6.82 (d, 1, J = 8.4, H-5), 6.84 (s, 1, H-3), 7.07 (d, J = 8.4, H-6), 7.31 (d, 2, J = 8, H-3′, H-5′), 8.11 (d, 2, J = 8, H-2′, H-6′). Found C, 76.32; H, 6.41. $C_{18}H_{18}O_3$ requires: C, 76.57; H, 6.43%.

6.3.14. 4-Allyl-2-methoxyphenyl 3-methoxybenzoate (4n). White crystal. Yield: 83%; mp 59–60 °C. IR: 1727 cm^{-1} (C═O). ^1H NMR ($CDCl_3$): δ 3.41 (d, 2, J = 6.6 Hz, –CH_2–), 3.80 (s, 3, –OCH_3), 3.88 (s, 3, –OCH_3), 5.01–5.23 (m, 2, H_2C═), 5.81–6.22 (m, 1, ═CH), 6.80 (d, 1, J = 8.6, H-5), 6.84 (s, 1, H-3), 7.07 (d, J = 8.6, H-6), 7.16 (d, 1, J = 8.8, H-4′), 7.40 (t, 1, J = 8.8, H-5′), 7.72 (s, 1, H-2′), 7.83 (d, J = 8.8, H-6′). Found C, 72.41; H, 6.06. $C_{18}H_{18}O_4$ requires: C, 72.47; H, 6.08%.

6.3.15. 4-Allyl-2-methoxyphenyl 4-methoxybenzoate (4o). White crystal. Yield: 85%; mp 93–94 °C. IR: 1731 cm^{-1} (C═O). ^1H NMR ($CDCl_3$): δ 3.40 (d, 2, J = 6.6 Hz, –CH_2–), 3.80 (s, 3, –OCH_3), 3.89 (s, 3, –OCH_3), 5.00–5.25 (m, 2, H_2C═), 5.81–6.24 (m, 1, ═CH), 6.80 (d, 1, J = 8.4, H-5), 6.84 (s, 1, H-3), 6.98 (d, 2, J = 8.9, H-3′, H-5′), 7.07 (d, J = 8.4, H-6), 8.17 (d, 2, J = 8.9, H-2′, H-6′). Found C, 72.32; H, 6.09. $C_{18}H_{18}O_4$ requires: C, 72.47; H, 6.08%.

6.3.16. 4-Allyl-2-methoxyphenyl 1-cyclohexanecarboxylate (4p). White crystal. Yield: 92%; mp 40–41 °C. IR: 1752 cm^{-1} (C═O). ^1H NMR ($CDCl_3$): δ 1.10–2.32 (m, 10, CH_2 cyclohexyl), 2.59 (m, 1, CH cyclohexyl), 3.39 (d, 2, J = 6.5 Hz, –CH_2–), 3.81 (s, 3, OCH_3), 5.02–5.25 (m, 2, H_2C═), 5.79–6.27 (m, 1, ═CH), 6.75 (d, 1, J = 8.4, H-5), 6.79 (s, 1, H-3), 6.95 (d, J = 8.4, H-6).

Found C, 74.48; H, 8.10. $C_{17}H_{22}O_3$ requires: C, 74.42; H, 8.08%.

6.3.17. 4-Allyl-2-methoxyphenyl 1-admantanecarboxylate (4q). White crystal. Yield: 89%; mp 89–90 °C. IR: 1738 cm^{-1} (C=O). ^1H NMR ($CDCl_3$): δ 1.76 (m, 9, CH, CH_2 adamantyl), 2.07 (m, 6, CH_2 adamantyl), 3.36 (d, 2, $J = 6.6$ Hz, $-CH_2-$), 3.78 (s, 3, OCH_3), 4.97–5.22 (m, 2, $H_2C=$), 5.82–6.20 (m, 1, =CH), 6.75 (d, 1, $J = 8.5$, H-5), 6.78 (s, 1, H-3), 6.90 (d, $J = 8.5$, H-6). Found C, 77.58; H, 8.03. $C_{21}H_{26}O_3$ requires: C, 77.27; H, 8.03%.

Acknowledgments

We express our sincere gratitude to Dr. F. Hadizadeh for software supporting and Dr. A. Sadeghian for statistical analysis studies.

References and notes

1. Raghavenra, H.; Diwakr, B. T.; Lokesh, B. R.; Naidu, K. A. *Prostaglandins, Leukotrienes Essential Fatty Acids* **2006**, *74*, 23–27.
2. Brash, A. R. *J. Biol. Chem.* **1999**, *274*, 23679–23682.
3. Kuhn, H.; Thiele, B. *J. FEBS Lett.* **1999**, *449*, 7–11.
4. Larsen, J. S.; Acosta, E. P. *Ann. Pharmacother.* **1993**, *27*, 898–903.
5. Schewe, T. *Biol. Chem.* **2002**, *383*, 365–374.
6. Kelavkar, U.; Glasgow, W.; Eling, T. E. *Curr. Urol. Rep.* **2002**, *3*, 207–214.
7. Kelavkar, U. P.; Cohen, C.; Kamitani, H.; Eling, T. E.; Badr, K. F. *Carcinogenesis* **2000**, *21*, 1777–1787.
8. Zhu, J.; Kilty, I.; Granger, H.; Gamble, E.; Qiu, Y. S.; Hattotuwa, K.; Elston, W.; Liu, W. L.; Liva, A.; Pauwels, R. A.; Kis, J. C.; De Rose, V.; Barnes, N.; Yeadon, M.; Jenkinson, S.; Jeffery, P. K. *Am. J. Respir. Cell Mol. Biol.* **2002**, *27*, 666–677.
9. Zhao, L.; Funk, C. D. *Trends Cardiovasc. Med.* **2004**, *14*, 191–195.
10. Cyrus, T.; Witztum, J. L.; Rader, D. J.; Tangirala, R.; Fazio, S.; Linton, M. F.; Funk, C. D. *J. Clin. Invest.* **1999**, 1597–1604.
11. Harats, D.; Shaish, A.; George, J.; Mulkins, M.; Kurihara, H.; Levkovitz, H.; Sigal, E. *Arteriosler. Thromb. Vasc. Biol.* **2000**, *20*, 2100–2105.
12. Sultana, C.; Shen, Y.; Rattan, V.; Kalra, V. J. *J. Cell. Phys.* **1996**, *167*, 467–487.
13. Setty, B. N.; Werner, M. H.; annun, Y. A.; Stuart, M. *J. Blood* **1992**, *80*, 2765–2773.
15. Chanez, P.; Bonnans, C.; Chavis, C.; Vachier, I. *Am. J. Respir. Crit. Care Med.* **2002**, *27*, 655–658.
16. Shappell, S. B.; Boeglin, W. E.; Olson, S. J.; Kasper, S.; Brash, A. R. *Am. J. Pathol.* **1999**, *155*, 235–245.
17. Hsi, L. C.; Wilson, L. C.; Eling, T. E. *J. Biol. Chem.* **2002**, *277*, 40549–40556.
18. Charlier, C.; Michaux, C. *Eur. J. Med. Chem.* **2003**, *38*, 645–659.
19. Markowitz, K.; Moynihan, M.; Liv, M.; Kim, S. *Oral Surg. Oral Pathol.* **1992**, *73*, 729–737.
20. IARC, Monograph, Evaluation of Carcinogenic Risk of Chemicals to Humans. Lyon, France, 1985; vol. 36, pp 75–97.
21. Wagner, H.; Jurcic, K.; Deininger, R. *Planta Med.* **1979**, *37*, 9–14.
22. Feng, J.; Lipton, J. M. *Neuropharmacology* **1987**, *26*, 1775–1778.
23. Hume, W. R. *J. Dent. Res.* **1983**, *62*, 1013–1015.
24. Moleyar, V.; Narasimham, P. *Int. J. Food Microbiol.* **1992**, *16*, 337–342.
25. Villani, F. J.; King, M. S. *Org. Syn. Coll.* **1963**, *4*, 88–89.
26. Thompson, J. D.; Gibson, T. J.; Plewniak, F.; Jeanmougin, F.; Higgins, D. G. *Nucleic Acids Res.* **1997**, *24*, 4876–4882.
27. http://us.expasy.org/.
28. ChemDraw® Ultra, *Chemical Structure Drawing Standard*, CambridgeSoft Corporation, 100 Cambridge Park Drive, Cambridge, MA 02140 USA, http://www.cambrigesoft.com.
29. HyperChem® Release 7, Hypercube Inc., http://www.hyper.com/.
30. Bakavoli, M.; Nikpour, M.; Rahimizadeh, M.; Saberi, M. R.; Sadeghian, H. *Bioorg. Med. Chem.* **2007**, *15*, 2120–2126.
31. Auto Dock Tools (ADT), *the Scripps Research Institute*, 10550 North Torrey Pines Road, La Jolla, CA 92037-1000, USA; (http://www.scripps.edu/pub/olson-web/doc/autodock/); Python, M.F.S.A programming language for software integration and development. *J. Mol. Graphics Mod.* **1999**, *17*, 57-61.
32. Morris, G. M.; Goodsell, D. S.; Halliday, R. S.; Huey, R.; Hart, W. E.; Belew, R. K.; Olson, A. J. *J. Comput. Chem.* **1998**, *19*, 1639–1662.
33. Sippl, W. *J. Comput. Aided Mol. Des.* **2000**, *14*, 559–572.
34. Dym, O.; Xenarios, I.; Ke, H.; Colicelli, J. *Mol. Pharmacol.* **2002**, *61*, 20–25.
35. http://sunfire.vbi.vt.edu/gcg/seqweb-guides/WebLab_Viewer.html.
36. Swiss-pdbViewer 3.6, *Glaxo Wellcome Experimental Research*, http://www.expasy.org/spdbv/.
37. DRAGON 2.1, *Milano Chemometrics and QSAR Research Group*, Department pf Environmental Sciences, P.za Della Scienza, 1-20126 Milano, Italy, http://www.disat.unimib.it/chem/.
38. Todeschini, R.; Consonni, V. *Handbook of Molecular Descriptors*; Wiley-VCH, Weinheim, Germany.
39. Kumar, R.; Pavithra, S. R.; Tatu, U. *J. Biosci.* **2007**, *32*, 531–536.
40. http://nihserver.mbi.ucla.edu/savs/.
41. Malterud, K. E.; Rydland, K. M. *J. Agric. Food Chem.* **2000**, *48*, 5576–5580.
42. Malterud, K. E.; Farbrot, T. L.; Huse, A. E.; Sund, R. B. *Pharmacology* **1993**, *47*, 77–85.
43. Skrzypczak-Jankun, E.; Bross, R.; Carroll, R. T.; Dunham, W. R.; Funk, M. O., Jr. *J. Am. Chem. Soc.* **2001**, *123*, 10814–10820.
44. Knapp, M. J.; Seebeck, F. P.; Klinman, J. P. *J. Am. Chem. Soc.* **2001**, *123*, 2931–2932.
45. Tomchick, D. R.; Phan, P.; Cymborowski, M.; Minor, W.; Holman, T. R. *Biochemistry* **2001**, *40*, 7509–7517.
46. Kyte, J.; Doolittle, R. F. *J. Mol. Biol.* **1982**, *157*, 105–132.